Maximum Likelihood Based Extended-Source Spatial Acquisition and Tracking for Planetary Optical Communications*

Haiping Tsou and Tsun-Yee Yan

Jet Propulsion Laboratory
California Institute of Technology
4800 Oak Grove Drive
Pasadena, CA 91109

ABSTRACT

This paper describes an extended-source spatial acquisition and tracking scheme for planetary optical communications. This scheme uses the Sun-lit Earth image as the beacon signal, which can be computed according to the current Sun-Earth-Probe angle from a pre-stored Earth image or a received snapshot taken by other Earth-orbiting satellite. Onboard the spacecraft, the reference image is correlated in the transform domain with the received image obtained from a detector array, which is assumed to have each of its pixels corrupted by an independent additive white Gaussian noise. The coordinate of the ground station is acquired and tracked, respectively, by an open-loop acquisition algorithm and a closed-loop tracking algorithm derived from the maximum likelihood criterion. As shown in the paper, the optimal spatial acquisition requires solving two nonlinear equations, or iteratively solving their linearized variants, to estimate the coordinate when translation in the relative positions of onboard and ground transceivers is considered. Similar assumption of linearization leads to the closed-loop spatial tracking algorithm in which the loop feedback signals can be derived from the weighted transform-domain correlation. Numerical results using a sample Sun-lit Earth image demonstrate that sub-pixel resolutions can be achieved by this scheme in a high disturbance environment.

Keywords: Laser-pointing; Extended-source image acquisition/tracking; Maximum likelihood estimation; Optical communications

1. INTRODUCTION

In optical communications, it is critical to maintain highly accurate pointing of optical transceivers on both ends of a communication link. Generally speaking, a beacon signal initiated from either end is required for spatial acquisition and continuously tracking if the relative position of transceivers is changing. For interplanetary space missions the beacon signal has to be initiated from the ground because the onboard transceiver usually has a much weaker power that can hardly afford to support a beacon signal. However, sending an Earth-based beacon laser signal over the long distance between the spacecraft and the Earth would still require a considerably large transmission power. An alternative is to use the Sun-lit Earth image as the beacon signal for spacecraft to determine the location of the ground transceiver. Unlike the high-power beacon laser used in the near-Earth missions as a point-source reference, the Sun-lit image has to be treated as an extended-source since, in general, it is asymmetric and extends several pixels on the focal plane of the detector array. Instead of the centroid type algorithms commonly used for a point-source with high signal-to-noise ratio, the nature of an extended-source warrants the use of correlation type algorithms having been developed for image acquisition in the applications such as image registration and moving target indication.[1,2]

The proposed spatial acquisition and tracking algorithms presented in this paper represent an extension to the above-mentioned work under random disturbances. The derivation is based on the maximum likelihood criterion between a received image and a reference image, where the uncertainties in-between are modeled as independent additive white Gaussian disturbances. The open-loop spatial acquisition scheme involves a correlation between received and referenced images in the transform domain. The reference image can be computed according to the current Sun-Earth-Probe angle from a pre-stored Earth image or a received snapshot taken by other Earth-orbiting

* The research described in this paper was carried out by the Jet Propulsion Laboratory, California Institute of Technology under contract with the National Aeronautic and Space Administration.

satellite. It is shown that the optimal spatial acquisition developed here requires solving two nonlinear equations in the transform domain to estimate the coordinate of the ground station, when the misalignment between the received and references images involves only a translation of coordinate. The suboptimal estimate exists by solving linearized version of the maximum likelihood criterion when computation complexity becomes a concern. A closed-loop image tracking algorithm motivated by the same maximum likelihood criterion is also developed for continuously tracking the translation movement between the onboard and ground transceivers. Because of the nature of tracking, the image tracking loop only requires solving two linear equations to continuously update its tracking.

In this paper, section 2 provides a general description of the mathematical model and the discrete Fourier transform of the image using the lexicographic representation. Section 3 derives the maximum likelihood estimator for spatial acquisition, followed by the derivation of the image tracking loop provided in section 4. The numerical results of a sample scenario to acquire a Sun-lit Earth beacon is provided in section 5, and section 6 summarizes this study and describes possible future research efforts.

2. MATHEMATICAL MODEL

2.1. Representation of Image

Based on the assumption of additive white Gaussian random disturbance mentioned previously, the extended-source image detected by an $M \times N$ array at time t_l, denoted as $r_l(m,n)$, can be represented by a sum of the source image, $s_l(m,n)$, and the random disturbance, $n_l(m,n)$, as follows

$$r_l(m,n) = s_l(m,n) + n_l(m,n), \qquad m = 0,1,\ldots,M-1, \quad n = 0,1,\ldots,N-1, \tag{1}$$

where $n_l(m,n)$ is a zero-mean Gaussian random variable with variance σ_l^2 for all m and n and is independent of each other.

The discrete Fourier transform of the received image at time t_l becomes

$$\mathcal{R}_l(m,n) = \mathcal{S}_l(m,n) + \mathcal{N}_l(m,n) \tag{2}$$

where the transform domain source image and random disturbance are

$$\mathcal{S}_l(m,n) = \sum_{p=0}^{M-1}\sum_{q=0}^{N-1} s_l(p,q) e^{-i2\pi\left(\frac{m}{M}p + \frac{n}{N}q\right)} \tag{3}$$

$$\mathcal{N}_l(m,n) = \sum_{p=0}^{M-1}\sum_{q=0}^{N-1} n_l(p,q) e^{-i2\pi\left(\frac{m}{M}p + \frac{n}{N}q\right)} \tag{4}$$

For notational convenience, the image matrix is represented in the lexicographic form such that

$$\vec{\mathcal{S}}_l = \begin{bmatrix} \mathcal{S}_l(0,0) \\ \mathcal{S}_l(0,1) \\ \vdots \\ \mathcal{S}_l(0,N-1) \\ \mathcal{S}_l(1,0) \\ \vdots \\ \mathcal{S}_l(1,N-1) \\ \vdots \\ \mathcal{S}_l(M-1,0) \\ \vdots \\ \mathcal{S}_l(M-1,N-1) \end{bmatrix} = \mathcal{F}\{\vec{s}_l\} = \mathcal{F}\{ \begin{bmatrix} s_l(0,0) \\ s_l(0,1) \\ \vdots \\ s_l(0,N-1) \\ s_l(1,0) \\ \vdots \\ s_l(1,N-1) \\ \vdots \\ s_l(M-1,0) \\ \vdots \\ s_l(M-1,N-1) \end{bmatrix} \} \tag{5}$$

where $\mathcal{F}\{\cdot\}$ denotes the discrete Fourier transform. Using the vector notation, from Eqs. (1) and (2), we have

$$\vec{r}_l = \vec{s}_l + \vec{n}_l$$

$$\vec{\mathcal{R}}_l = \vec{\mathcal{S}}_l + \vec{\mathcal{N}}_l$$

2.2. Translation Movement

If the extended source makes a translation movement within the field of view of the detector array between t_l and t_{l+1} by the amount of x_l and y_l pixels along the x-axis and y-axis, respectively, the image at t_{l+1} is related to the original image at t_l by

$$s_{l+1}(m,n) = s_l(m - x_l, n - y_l) \tag{6}$$

or, in the lexicographic form, as

$$\vec{s}_{l+1} \triangleq \mathbb{L}_{x_l,y_l}\{\vec{s}_l\} \tag{7}$$

where $\mathbb{L}_{x,y}\{\cdot\}$ is defined as a translation operator which move the operand by a translation vector (x,y).

In the transform domain, it can be easily shown that the effect of translation movement becomes

$$\mathcal{S}_{l+1}(m,n) = \mathcal{S}_l(m,n)e^{i\theta_{m,n,l}} \tag{8}$$

where

$$\theta_{m,n,l} = -2\pi\left(\frac{m}{M}x_l + \frac{n}{N}y_l\right) \tag{9}$$

is the phase introduced to the pixel (m,n) of the transform domain image due to the translation of coordinate from t_l to t_{l+1}.

Hence, from Eq. (2), the transform domain received image at time t_{l+1} can be expressed by

$$\mathcal{R}_{l+1}(m,n) = \mathcal{S}_l(m,n)e^{i\theta_{m,n,l}} + \mathcal{N}_{l+1}(m,n) \tag{10}$$

or, in the lexicographic form, as

$$\vec{\mathcal{R}}_{l+1} = \vec{\mathcal{S}}_l \cdot e^{i\Theta(x_l,y_l)} + \vec{\mathcal{N}}_{l+1} \tag{11}$$

where "$\cdot$" denotes entry-by-entry product of two vectors and

$$e^{i\Theta(x_l,y_l)} = \begin{bmatrix} e^{i\theta_{0,0,l}} \\ e^{i\theta_{0,1,l}} \\ \vdots \\ e^{i\theta_{0,N-1,l}} \\ e^{i\theta_{1,0,l}} \\ \vdots \\ e^{i\theta_{1,N-1,l}} \\ \vdots \\ e^{i\theta_{M-1,0,l}} \\ \vdots \\ e^{i\theta_{M-1,N-1,l}} \end{bmatrix} \tag{12}$$

with $\theta_{m,n,l}$ being given in Eq. (9).

3. MAXIMUM LIKELIHOOD ESTIMATE OF TRANSLATION VECTOR

From Eq. (1), a maximum likelihood estimator will compare the received image $\vec{r}_{l+1}$ against the reference image $\vec{s}_l$ and declare the estimated translation vector $(\hat{x}_l, \hat{y}_l)$ if

$$f(\vec{r}_{l+1} \mid \hat{x}_l, \hat{y}_l) = \max_{\{(x_l,y_l)\}} f(\vec{r}_{l+1} \mid x_l, y_l) \tag{13}$$

where

$$f(\vec{r}_{l+1} \mid x_l, y_l) = \frac{1}{\left(\sqrt{2\pi}\sigma_l\right)^{MN}} e^{-\frac{1}{2\sigma_l^2}\|\vec{r}_{l+1} - \vec{s}_{l+1}\|^2} \tag{14}$$

is the conditional probability density function of $\vec{r}_{l+1}$ given that the translation vector is (x_l, y_l). The maximum likelihood criterion stated in Eq. (13) is equivalent to

$$\min_{\{(x_l,y_l)\}} \| \vec{r}_{l+1} - \vec{s}_{l+1} \|^2 = \min_{\{(x_l,y_l)\}} \| \vec{r}_{l+1} - \mathbb{L}_{x_l,y_l}\{\vec{s}_l\} \|^2 = \| \vec{r}_{l+1} - \mathbb{L}_{\hat{x}_l,\hat{y}_l}\{\vec{s}_l\} \|^2 \tag{15}$$

Since the Fourier transform $\frac{1}{MN}\mathcal{F}\{\cdot\}$ is unitary, under $\mathcal{L}_2$ norm, we have

$$\begin{aligned} \| \vec{r}_{l+1} - \vec{s}_{l+1} \|^2 &= \frac{1}{MN} \| \mathcal{F}\{\vec{r}_{l+1}\} - \mathcal{F}\{\vec{s}_{l+1}\} \|^2 \\ &= \frac{1}{MN} \| \vec{R}_{l+1} - \vec{S}_l \cdot e^{i\Theta(x_l,y_l)} \|^2 \end{aligned} \tag{16}$$

Expanding the above expression leads to

$$\| \vec{R}_{l+1} - \vec{S}_l \cdot e^{i\Theta(x_l,y_l)} \|^2 = \sum_{m=0}^{M-1} \sum_{n=0}^{N-1} \left\{ |\mathcal{R}_{l+1}(m,n)|^2 + |\mathcal{S}_l(m,n)|^2 - 2|w_l(m,n)| \cos(\xi_{m,n,l} - \theta_{m,n,l}) \right\} \tag{17}$$

where

$$w_l(m,n) \triangleq \mathcal{R}_{l+1}(m,n)\mathcal{S}_l^*(m,n) = |w_l(m,n)| e^{i\xi_{m,n,l}} \tag{18}$$

is the pixel-by-pixel product of the transform-domain received image $\mathcal{R}_{l+1}(m,n)$ and the complex conjugate of the transform-domain reference image $\mathcal{S}_l(m,n)$. By substituting Eq. (18) into Eq. (17) and removing constant terms not affected by the choice of (x_l, y_l), the maximum likelihood criterion stated in Eq. (15) can finally be reduced to

$$\max_{\{(x_l,y_l)\}} \left\{ \frac{1}{MN} \sum_{m=0}^{M-1} \sum_{n=0}^{N-1} |w_l(m,n)| \cos(\xi_{m,n,l} - \theta_{m,n,l}) \right\} = \| \vec{r}_{l+1} - \mathbb{L}_{\hat{x}_l,\hat{y}_l}\{\vec{s}_l\} \|^2 \tag{19}$$

Note that the likelihood function to be maximized in Eq. (19) can be rewritten as

$$\mathrm{Re}\left\{ \frac{1}{MN} \sum_{m=0}^{M-1} \sum_{n=0}^{N-1} \mathcal{R}_{l+1}(m,n)\mathcal{S}_l^*(m,n) e^{-i\theta_{m,n,l}} \right\} \tag{20}$$

where $\mathrm{Re}\{\cdot\}$ represents the real part of a complex quantity. It is clearly indicated that the likelihood function involves the average over all pixels of the pixel-wise multiplied received and reference images in the transform domain, as well as the phase to be estimated.

Taking the partial derivatives of Eq. (20) with respect to x_l and y_l and equating them to zero, we have

$$\begin{aligned} &\sum_{m=0}^{M-1} \sum_{n=0}^{N-1} m|w_l(m,n)| \sin(\xi_{m,n,l} - \theta_{m,n,l}) = 0 \\ &\sum_{m=0}^{M-1} \sum_{n=0}^{N-1} n|w_l(m,n)| \sin(\xi_{m,n,l} - \theta_{m,n,l}) = 0 \end{aligned} \tag{21}$$

which form a set of nonlinear equations to be solved for the maximum likelihood estimates of x_l and y_l.

If the extended-source is close to being acquired, the phase differences, $(\xi_{m,n,l} - \theta_{m,n,l})$, will be small and the approximation of $\sin(x) \approx x$ can be applied to Eq. (21), rendering the suboptimal linear estimator

$$\begin{aligned} \sum_{m=0}^{M-1} \sum_{n=0}^{N-1} m|w_l(m,n)|\xi_{m,n,l} &= \sum_{m=0}^{M-1} \sum_{n=0}^{N-1} m|w_l(m,n)|\theta_{m,n,l} \\ \sum_{m=0}^{M-1} \sum_{n=0}^{N-1} n|w_l(m,n)|\xi_{m,n,l} &= \sum_{m=0}^{M-1} \sum_{n=0}^{N-1} n|w_l(m,n)|\theta_{m,n,l} \end{aligned} \tag{22}$$

The estimated vector $(\hat{x}_l, \hat{y}_l)$ obtained from solving this suboptimal linear maximum likelihood criterion must satisfy

$$\begin{aligned}
-\frac{1}{2\pi}\sum_{m=0}^{M-1}\sum_{n=0}^{N-1} m|w_l(m,n)|\xi_{m,n,l} &= x_l \sum_{m=0}^{M-1}\sum_{n=0}^{N-1} m\frac{m}{M}|w_l(m,n)| + y_l \sum_{m=0}^{M-1}\sum_{n=0}^{N-1} m\frac{n}{N}|w_l(m,n)| \\
-\frac{1}{2\pi}\sum_{m=0}^{M-1}\sum_{n=0}^{N-1} n|w_l(m,n)|\xi_{m,n,l} &= x_l \sum_{m=0}^{M-1}\sum_{n=0}^{N-1} n\frac{m}{M}|w_l(m,n)| + y_l \sum_{m=0}^{M-1}\sum_{n=0}^{N-1} n\frac{n}{N}|w_l(m,n)|
\end{aligned} \tag{23}$$

The solution of Eq. (23) is identical to algorithms derived by Kuglin and Pearson.[1,2]

4. IMAGE TRACKING LOOP

To maximize the likelihood function of acquiring an image disturbed by additive white Gaussian noise involves a comparison of the received image against the reference image. However, for image tracking, it is the correlation between the transform-domain received image $\mathcal{R}_{l+1}(m,n)$ and the estimated translated reference image

$$\hat{\mathcal{R}}_{l+1}(m,n) = \mathcal{S}_l(m,n)e^{i\hat{\theta}_{m,n,l}}$$

to be continuously maximized. The pixel-wise product of $\mathcal{R}_{l+1}(m,n)$ and $\hat{\mathcal{R}}^*_{l+1}(m,n)$ can be expressed by

$$\begin{aligned}
C_{l+1}(m,n) &\triangleq \mathcal{R}_{l+1}(m,n)\mathcal{S}^*_l(m,n)e^{-i\hat{\theta}_{m,n,l}} \\
&= |\mathcal{S}_l(m,n)|^2 e^{i\phi_{m,n,l}} + \mathcal{N}_{l+1}(m,n)\mathcal{S}^*_l(m,n)e^{-i\hat{\theta}_{m,n,l}}
\end{aligned} \tag{24}$$

where $\hat{\theta}_{m,n,l}$ is the estimate of $\theta_{m,n,l}$ and the estimation error is

$$\begin{aligned}
\phi_{m,n,l} &= \theta_{m,n,l} - \hat{\theta}_{m,n,l} \\
&= -2\pi\left[\frac{m}{M}(x_l - \hat{x}_l) + \frac{n}{N}(y_l - \hat{y}_l)\right] \\
&\triangleq -2\pi\left(\frac{m}{M}\Delta_x + \frac{n}{N}\Delta_y\right)
\end{aligned} \tag{25}$$

where $\hat{x}_l$ and $\hat{y}_l$ are estimates of x_l and y_l, respectively, and Δ_x and Δ_y are the associated estimate errors. The average of $C_{l+1}(m,n)$ over all pixels results in the correlation between $\mathcal{R}_{l+1}(m,n)$ and $\hat{\mathcal{R}}_{l+1}(m,n)$.

According to the maximum likelihood criterion derived in the previous section, the real part of Eq. (24) shall be maximized over the entire detector array, rendering the maximum likelihood estimates $\hat{x}_l$ and $\hat{y}_l$ which maximize

$$\sum_{m=0}^{M-1}\sum_{n=0}^{N-1} \mathrm{Re}\{C_{l+1}(m,n)\} \tag{26}$$

By following the derivation given in the previous section, it turns out that $\hat{x}_l$ and $\hat{y}_l$ can be obtained by solving a set of two nonlinear equations which are formed by setting the partial derivatives of Eq. (26) with respect to $\hat{x}_l$ and $\hat{y}_l$ to be zero. In deriving the image tracking algorithm to continuously update the estimates, two loop feedback signals can be similarly formed as the partial derivatives of Eq. (26) with respect to Δ_x and Δ_y, rendering

$$\begin{aligned}
\varepsilon_x &\triangleq \frac{\partial}{\partial\Delta_x}\sum_{m=0}^{M-1}\sum_{n=0}^{N-1} \mathrm{Re}\{C_{l+1}(m,n)\} \\
&= \frac{2\pi}{M}\sum_{m=0}^{M-1}\sum_{n=0}^{N-1} m|\mathcal{S}_l(m,n)|^2 \sin(\phi_{m,n,l}) + \sum_{m=0}^{M-1}\sum_{n=0}^{N-1}\mathcal{N}^{(x)}_{l,eff}(m,n)
\end{aligned} \tag{27}$$

$$\begin{aligned}
\varepsilon_y &\triangleq \frac{\partial}{\partial\Delta_y}\sum_{m=0}^{M-1}\sum_{n=0}^{N-1} \mathrm{Re}\{C_{l+1}(m,n)\} \\
&= \frac{2\pi}{N}\sum_{m=0}^{M-1}\sum_{n=0}^{N-1} n|\mathcal{S}_l(m,n)|^2 \sin(\phi_{m,n,l}) + \sum_{m=0}^{M-1}\sum_{n=0}^{N-1}\mathcal{N}^{(y)}_{l,eff}(m,n)
\end{aligned} \tag{28}$$

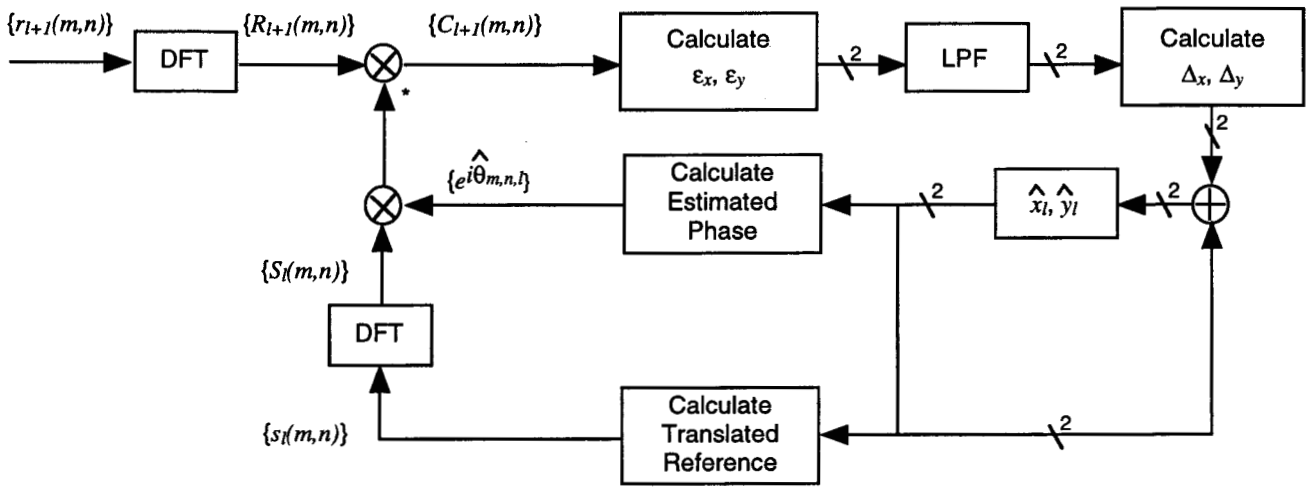

Figure 1. The Extended-Source Image Tracking Loop.

where

$$\mathcal{N}_{l,eff}^{(x)}(m,n) = \frac{\partial}{\partial \Delta_x}\mathrm{Re}\left\{\mathcal{N}_{l+1}(m,n)\mathcal{S}_l^*(m,n)e^{-i\hat{\theta}_{m,n,l}}\right\}$$

$$\mathcal{N}_{l,eff}^{(y)}(m,n) = \frac{\partial}{\partial \Delta_y}\mathrm{Re}\left\{\mathcal{N}_{l+1}(m,n)\mathcal{S}_l^*(m,n)e^{-i\hat{\theta}_{m,n,l}}\right\}$$

constitute the effective noises in the loop operation. Equations (27) and (28) characterize the relationship between the estimate errors, Δ_x and Δ_y, and the loop feedback signals, ε_x and ε_y. However, to solve for Δ_x and Δ_y from these nonlinear equations can be a quite challenging task, especially for the limited computing capacity of the onboard processor. With a reasonable linear assumption valid when the phase error $\phi_{m,n,l}$ remains small during the tracking mode, one can substitute Eq. (25) for $\sin(\phi_{m,n,l})$ in Eqs. (27) and (28). The resulting simultaneous equations are linear for Δ_x and Δ_y and can be easily solved, yielding

$$\Delta_x = \frac{C_n\mathbb{E}[\varepsilon_x] - C_{mn}\mathbb{E}[\varepsilon_y]}{C_mC_n - C_{mn}^2} \tag{29}$$

$$\Delta_y = \frac{C_{mn}\mathbb{E}[\varepsilon_x] - C_m\mathbb{E}[\varepsilon_y]}{C_{mn}^2 - C_mC_n} \tag{30}$$

where $\mathbb{E}[\cdot]$ denotes the statistical expectation and

$$C_m \triangleq \frac{4\pi^2}{M^2}\sum_{m=0}^{M-1}\sum_{n=0}^{N-1} m^2|\mathcal{S}_l(m,n)|^2$$

$$C_n \triangleq \frac{4\pi^2}{N^2}\sum_{m=0}^{M-1}\sum_{n=0}^{N-1} n^2|\mathcal{S}_l(m,n)|^2$$

$$C_{mn} \triangleq \frac{4\pi^2}{MN}\sum_{m=0}^{M-1}\sum_{n=0}^{N-1} mn|\mathcal{S}_l(m,n)|^2$$

are coefficients that can be calculated from the reference image of the previous iteration at t_l.

An extended-source image tracking loop structure can be realized based upon the above discussion and is depicted in Fig. 1. The transform-domain received image $\{\mathcal{R}_{l+1}(m,n)\}$ is first multiplied pixel-wise with a properly translated transform-domain reference image established according to the estimate $(\hat{x}_l, \hat{y}_l)$ from the previous iteration at t_l. After being averaged over the extended-source, the correlation result is used to compute the loop feedback signals, ε_x and ε_y. It is important to note that these two loop feedback signals can not be calculated from Eqs. (27) and (28) since

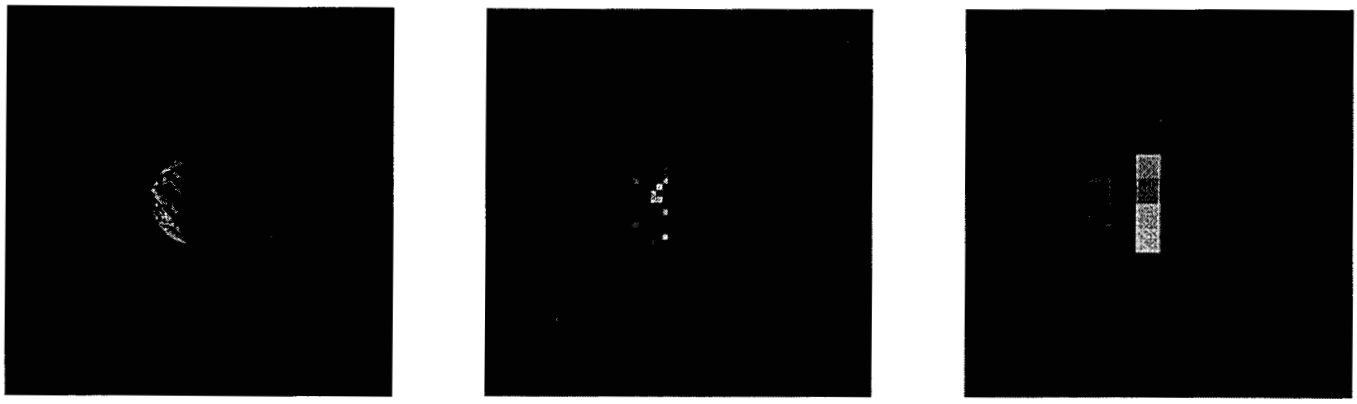

(a) (b) (c)

Figure 2. The Extended-Source Images: (a) original image of size 256 × 256, (b) reference image of size 64 × 64, and (c) detected image of size 16 × 16.

Δ_x and Δ_y are not readily accessible for the partial derivatives. However, by carefully examining Eqs. (24) and (25), it turns out that both ε_x and ε_y can be directly calculated from $C_{l+1}(m,n)$ as the following weighted sums

$$\varepsilon_x = \frac{2\pi}{M} \sum_{m=0}^{M-1} \sum_{n=0}^{N-1} m\mathrm{Im}\{C_{l+1}(m,n)\} \tag{31}$$

$$\varepsilon_y = \frac{2\pi}{N} \sum_{m=0}^{M-1} \sum_{n=0}^{N-1} n\mathrm{Im}\{C_{l+1}(m,n)\} \tag{32}$$

where $\mathrm{Im}\{\cdot\}$ represents the imaginary part of a complex quantity. The subsequent calculation of Δ_x and Δ_y from ε_x and ε_y is straightforward as indicated in Eqs. (29) and (30), except that the statistical averages are replaced by time averages performed by low pass filters. The calculated Δ_x and Δ_y will be used to update the movement estimates through an accumulator, such that

$$\hat{x}_{l+1} = \hat{x}_l + \Delta_x \tag{33}$$

$$\hat{y}_{l+1} = \hat{y}_l + \Delta_y \tag{34}$$

The updated accumulator contents will be used to calculate the estimate $\hat{\theta}_{m,n,l+1}$ and prepare the translated reference image for the next loop iteration at t_{l+1}.

5. NUMERICAL RESULTS

The spatial acquisition scheme presented in section 3 has been simulated for different Sun-lit Earth images compressed from a size of 256 × 256 to a size of 64 × 64. These reference images are assumed to have uniform albedo. The received images used for simulation are assumed to be detected by a 16 × 16 CCD array and corrupted by additive white Gaussian disturbances such that the average signal-to-noise ratio

$$\left(\frac{S}{N}\right) = \frac{1}{\sqrt{MN}} \frac{\| \vec{s}_l \|}{\sigma_l} = 1 \tag{35}$$

Figure 2 shows the images used in one of the simulated scenarios.

During the acquisition, the reference image is scaled down to a 16 × 16 image to match the size of the received image. The acquisition process as suggested by Eq. (21) requires $M \times N$ terms of summation for each of the simultaneous equations. The actual size of computation can be reduced by forming partial sums of Eq. (21) such

Computation Index		Estimated Coordinate		Actual Coordinate	
M_c	N_c	Rows	Columns	Rows	Columns
4	4	3.75	-3.14	3.625	-2.82
6	6	3.55	-2.84		
8	8	3.55	-2.81		

Table 1. Estimated Ground Station Coordinate during Acquisition

that

$$g_1(x_l, y_l) = \sum_{m=0}^{M_c-1} \sum_{n=0}^{N_c-1} m|w_l(m,n)| \sin(\xi_{m,n,l} - \theta_{m,n,l})$$
$$g_2(x_l, y_l) = \sum_{m=0}^{M_c-1} \sum_{n=0}^{N_c-1} n|w_l(m,n)| \sin(\xi_{m,n,l} - \theta_{m,n,l}) \tag{36}$$

where $1 \leq M_c \leq M$ and $1 \leq N_c \leq N$. Solving $g_1(x_l, y_l) = 0$ and $g_2(x_l, y_l) = 0$ requires a reduced computation size of $M_c \times N_c$ results at the expense of getting suboptimal solutions. Theoretically, as M_c and N_c increase, this reduced size computation gives better estimation. This implies that Eq. (36) can be applied iteratively to direct the receiving optics towards the real target. The algorithm will eventually be terminated when estimates converge as M_c and N_c increase.

In our simulation, the iterative approach illustrated in Eq. (36) is applied to the linear estimator given in Eq. (22). Table 1 shows the estimated coordinate as the computation indices M_c and N_c increase. The estimates are refined to (3.55,-2.81) relative to the 16×16 CCD array, which translates to a sub-pixel accuracy of less than 2 and 1 percent in the respective direction of the original reference image.

6. CONCLUSION

This paper describes an extended-source spatial acquisition and tracking scheme for planetary optical communications, which uses the Sun-lit Earth image as the reference signal. The uncertainties between the reference image and the received image are modeled as additive white Gaussian disturbances. It has been shown that under these assumptions the optimum spatial acquisition process derived from the maximum likelihood criterion requires solving two nonlinear equations to estimate the coordinate of the ground station from the received camera image in the transform domain. The optimal solution can also be obtained iteratively using linear approximations. Similar assumption of linearization leads to the closed-loop spatial tracking algorithm in which the loop feedback signals can be derived from the weighted transform-domain correlation between the received image and the reference image. With recent advances in photonic and computing technologies, integrated acquisition and tracking becomes possible as a portion of the detector sub-array can be dedicated to perform tracking, which minimizes the handover and possible alignment problems between acquisition and tracking. Numerical results using a sample Sun-lit Earth image demonstrate that sub-pixel resolutions can be achieved by this maximum-likelihood based spatial acquisition scheme in a high disturbance environment. More numerical results for the image tracking performance is currently under simulation and will be included in a future paper.

There are several areas remain for further investigation. For example, the relative movement considered in this paper is limited to translation. Future work will take rotation into consideration as well. Furthermore, the assumption of independent white Gaussian disturbance in each pixel holds for specific cases such as the atmosphere scintillation, however, it may not be valid for spatially correlated case such as the albedo variations and the image obtained from sub-pixel scanning.

REFERENCES

1. C. D. Kuglin and D. C. Hines, "The phase correlation image alignment method," *Proc. Int. Conf. on Cybernetics and Society* , pp. 163–165, 1975.
2. J. J. Pearson, D. C. Hines, S. Golosman, and C. D. Kuglin, "Video-rate image correlation processor," *Proc. SPIE* **119,** Application of Digital Image Processing, IOCC 1977, pp. 197–205, 1977.